COMMUNICATION

ChemComm
www.rsc.org/chemcomm

TEM stereo-imaging of mesoporous zeolite single crystals†

Astrid Boisen,*[ab] Iver Schmidt,[a] Anna Carlsson,[a] Søren Dahl,[a] Michael Brorson[a] and Claus J. H. Jacobsen[a]

[a] *Haldor Topsøe A/S, Nymøllevej 55, DK-2800 Lyngby, Denmark. E-mail: asb@topsoe.dk; Fax: +45 4527 2999; Tel: +45 4527 2680*

[b] *Interdisciplinary Research Center for Catalysis (ICAT), Dept. of Chemical Engineering, Technical University of Denmark, DK-2800 Lyngby, Denmark*

Received (in Cambridge, UK) 23rd December 2002, Accepted 27th February 2003
First published as an Advance Article on the web 14th March 2003

Mesoporous zeolite single crystals with intracrystalline mesopores and metal oxide particles located in the zeolite mesopore are characterised by direct TEM stereo-imaging.

Zeolites find widespread use both in separation processes as sorbents and as heterogeneous catalysts.[1] The presence of micropores (diameter < 2.0 nm) with a well-defined pore size and pore geometry is of major importance in these industrial applications.[2] The pore size and pore geometry is determined by the crystal structure of the zeolite and today a wide range of zeolites with different crystal structures are available. However, in several applications it has been shown that the presence of larger pores, mesopores, is desirable in order to increase the rate of diffusion in the zeolite crystals.[3–5] Usually, the desired mesoporosity is introduced by post-treatment of the crystallized zeolite. Typical procedures involve steaming at elevated temperatures, or acid leaching,[6] and mesopores result from the extraction of aluminium from the crystalline zeolite. Partial disintegration of the zeolite crystals occurs and extra-framework aluminium species are created.

Here, we show how it is possible to directly visualize the pore system of mesoporous zeolite single crystals for an MFI zeolite with mesopores generated by carbon nanotube templating. At the same time, we show how TEM stereo-imaging can be used to distinguish metal particles located in the mesopores from metal particles located at the external surface of the zeolite crystals. This distinction would not be possible by conventional TEM or by any other characterization method.

Recently, the mesopores generated by post-treatments were characterized by 3D transmission electron microscopy (TEM).[7] Generally, the extraction processes do not lead to a well-defined pore system, they are at least partially destructive to the zeolite crystals, and they generate poorly characterized aluminium species. Furthermore, they are not applicable to high-silica zeolites, since they have little or even no aluminium content.

We have developed an alternative approach for the preparation of mesoporous zeolites[8] which involves crystallization in an inert, removable matrix, *e.g.*, carbon black or multi-wall carbon nanotubes (MWNTs). This results in growth of the large individual single crystals around the carbon particles of the matrix. By removal of the carbon by combustion, zeolite single crystals containing randomly oriented intracrystalline mesopores are formed. It is essential that the zeolite gel is synthesised in the void between the carbon particles. This can be achieved by sequential impregnations of the carbon matrix with the individual synthesis gel components.

Very uniform and straight mesopores are obtained using MWNTs as a mesopore forming agent.[9] The use of MWNTs as template offers a high degree of control over the diameters and spatial arrangement of mesopores in solid materials, a control not offered by any other currently available synthesis method.

Multi-wall carbon nanotubes (MWNT) were supplied by Hyperion Catalysis International, MA, USA. The nanotubes were purified by reflux in concentrated hydrochloric acid for 24 hours. This purification step was repeated until the hydrochloric acid was no longer colored by impurities (mostly iron) from the nanotubes (typically 5–6 times) which reduces the iron content from 1.2 to < 0.1 wt%. Mesoporous ZSM-5 was prepared by sequential, incipient wetness impregnation of the MWNT (average diameter 12 nm) with each of the gel components. Sodium aluminate ($NaAlO_2$, 0.16 g) was dissolved in a mixture of a 40-wt. % aqueous solution of tetrapropylammonium hydroxide (TPAOH, 14.8 g) and H_2O (2.5 g). Ethanol (13.8 g) was added and the resulting solution was impregnated onto the MWNT (12.1 g). After evaporation of the ethanol at room temperature, the MWNTs were impregnated with tetraethylorthosilicate (TEOS, 16.6 g). The sample was digested for 16 hours, and then impregnated with TPAOH (40%) and H_2O (1 : 10) to 20% excess (compared to incipient wetness). The impregnated MWNT material was transferred to an autoclave containing enough water to produce saturated steam and crystallized at 180 °C for 70 h. After the hydrothermal crystallization, the composite was suspended in water, filtered by suction, and re-suspended in water. This was repeated four times. Then the sample was washed with ethanol and subsequently dried at 110 °C for 24 h. The carbon nanotubes were completely removed by controlled combustion in air in a muffle furnace at 600 °C for 20 h. In this way a brownish crystalline powder was obtained. From the XRPD patterns obtained with the setup described previously[10] it was found that the sample contained only MFI-type zeolite and iron oxide. The iron oxide (< 5 wt. %) stems from the carbon nanotube material and is the reason for the brownish appearance of the zeolite sample.

Pore size distributions were obtained from isotherms measured with a Quantachrome Autosorb-3 using N_2 or Ar as adsorbant at 77 K. N_2 adsorption/desorption isotherms are shown in Fig. 1.

BJH analysis of the desorption isotherms revealed pore size distributions with mesopores in the range of 6–15 nm radius corresponding to the diameter of the carbon nanotubes. The external surface area (including the mesopore surface area) was found to be ~ 120 m² g⁻¹ by the t-method. This is 1/3 of the total BET surface area of ~ 360 m² g⁻¹.

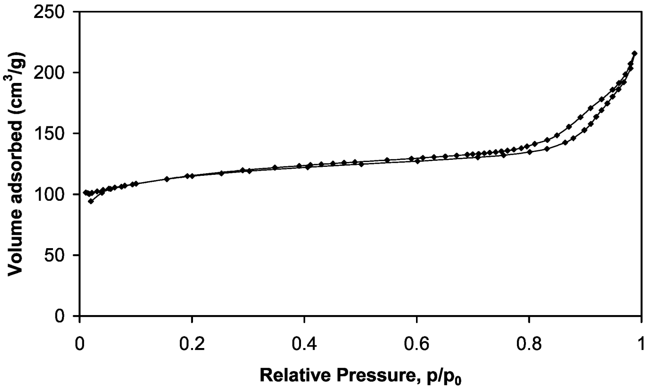

Fig. 1 N_2 adsorption and desorption isotherms at 77 K for a mesoporous HZSM-5 zeolite.

---

† Electronic supplementary information (ESI) available: a sequence of images. See http://www.rsc.org/suppdata/cc/b2/b212646j/

DOI: 10.1039/b212646j

This journal is © The Royal Society of Chemistry 2003

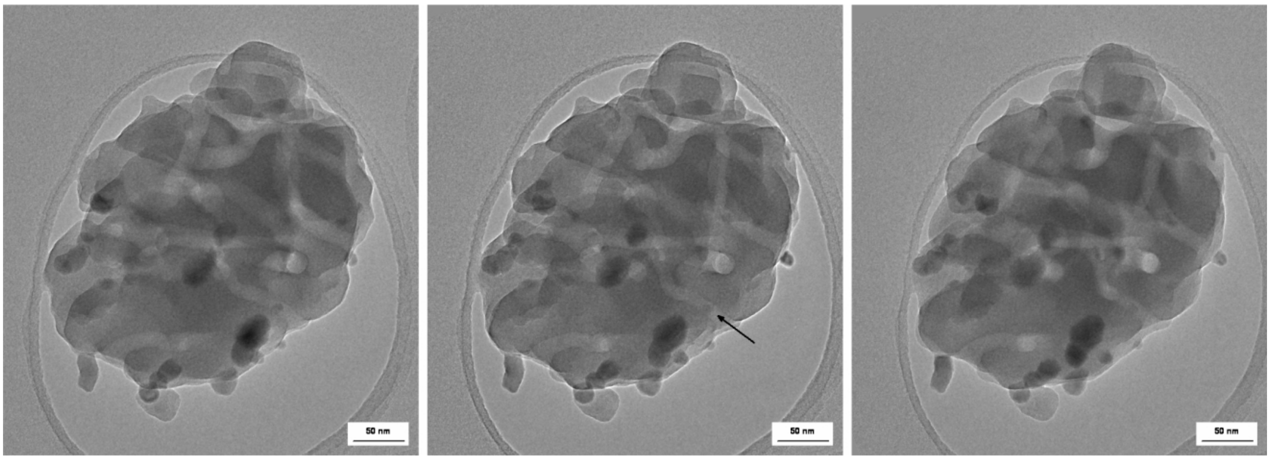

Fig. 2 TEM stereo images of a HZSM-5 zeolite single crystal with intra-crystalline mesopores created by crystallisation around multi-wall carbon nanotubes. They can be viewed in pairs, *e.g.*, with stereo glasses. The arrow is pointing towards an iron oxide particle located inside the mesopore system. Most other iron oxide particles are situated at the external surface of the zeolite single crystal.

A sample was prepared for transmission electron microscopy (TEM) by dispersing it in ethanol and placing a drop of the suspension on a copper grid coated with lacey carbon film. TEM images were recorded with a Philips CM200 FEG Ultrathin operated at 200 kV, and equipped with a Gatan Multiscan CCD model 794. The crystal sizes varied between 0.25 and 1.0 µm. A representative crystal was selected for recording the tilt series, which consisted of 20 images covering a specimen tilt from −20° to +18° (the maximum tilt range of this high-resolution microscope). The tilt series was recorded at 30 000 times magnification, corresponding to 0.57 nm pixel^{-1}. Due to the low magnification lattice fringes are not visible in the images, but electron diffraction patterns (not shown) verified that the crystal is a single crystal. The 20 images were aligned using cross-correlation between consecutive images, and rotated to make the tilt axis vertical. Three images from the tilt series are shown in Fig. 2.†

A metal oxide particle located in the mesopore system is marked with an arrow. Several other metal oxide particles are located at the zeolite surface. The mesopores are seen as well-defined channels extending through the entire crystal. The stereo images of the crystal can contribute to the understanding of the 3-dimensional ordering of the structure, allowing a distinction between metal oxide particles located in the mesopores of the zeolite crystal and metal oxide particles on the external surface of the crystal. In conventional TEM, the 3-dimensional structure is projected into a 2-dimensional image and the information in the third dimension is lost. TEM stereo-imaging helps to visualise the mesopores, and directly provides information about the size, shape, connectivity, tortuosity, and orientation of the pores. Thus, to model the diffusion of reactants and products in mesoporous zeolite catalysts, TEM stereo-imaging is a unique tool. TEM stereo-imaging also enables direct imaging of metal oxide particles located in the mesopores and on the external surface of mesoporous zeolite crystals.

3D TEM (tomography) was recently used to establish the location of a silver particle in the micropores of a NaY zeolite.[11,12] Tomography allows 3D images of the sample to be obtained. However, it requires a tilting range of approximately +70° to −70°.

Particularly in bifunctional catalysis, mesoporous zeolites are promising. Typically, such catalysts would contain an acid site (residing in the zeolite micropores) and a hydrogenating/dehydrogenating site introduced through *e.g.*, a metallic component. In these catalysts, it would be desirable to locate the metal particles inside the zeolite mesopores rather than on the external surface of the zeolite crystals, thus creating a shorter distance between the two catalytic functionalities.

The iron oxide particles that were present in both the zeolite mesopores and on the zeolite surface stemmed from the carbon nanotube material in which they were originally encapsulated as impurities. The activity of bifunctional catalysts is sensitive to both the structural features of the zeolite and the dispersion degree and particle morphology of the metal component, this shows that metal particles can be introduced into zeolite mesopores by initially dispersing them on the carbon matrix.

At the same time, changing the nature of the carbon matrix, *e.g.*, by controlling the diameter of the carbon nanotubes, allows design of the zeolite mesopore system.

In the recent past, it has been shown that mesoporous single crystals constitute a new family of materials that also include non-zeolitic materials. Use of a block copolymer, allowed crystallization of mesoporous single crystal particles of a mixed niobium-tantalum oxide[13,14] and similarly selective dissolution of a silica template yielded mesoporous chromium(III) oxide single crystals.[15] 2D TEM imaging techniques will not allow determination of the properties relevant in solid–gas or solid–liquid processes. Here, TEM Stereo-imaging or 3D TEM serves its full potential.

Notes and references

1 P. A. Jacobs and J. A. Martens, *Stud. Surf. Sci. Catal.*, 1991, **58**, 445.
2 C. C. Freyhardt, M. Tsapatis, R. F. Lobo, K. J. Balkus Jr. and M. E. Davis, *Nature*, 1996, **381**, 295.
3 I. Schmidt, A. Krogh, K. Wienberg, A. Carlsson, M. Brorson and C. J. H. Jacobsen, *Chem. Commun.*, 2000, 2157.
4 J. Houzvicka, C. J. H. Jacobsen and I. Schmidt, *Stud. Surf. Sci Catal.*, 2001, **135**, 158.
5 S. van Donk, A. Broersma, O. L. J. Gijzeman, J. A. van Bokhoven, J. H. Bitter and K. P. de Jong, *J. Catal.*, 2001, **204**, 272.
6 G. R. Meima, *CATTECH*, 1998, **2**, 5.
7 A. H. Janssen, A. J. Koster and K. P de Jong, *Angew. Chem., Int. Ed. Engl.*, 2001, **40**, 1102.
8 C. J. H. Jacobsen, C. Madsen, J. Houzvicka, I. Schmidt and A. Carlsson, *J. Am. Chem. Soc.*, 2000, **122**, 7116.
9 I. Schmidt, A. Boisen, E. Gustavsson, K. Ståhl, S. Pehrson, S. Dahl, A. Carlsson and C. J. H. Jacobsen, *Chem. Mater.*, 2001, **13**, 4416.
10 C. Madsen and C. J. H. Jacobsen, *Chem. Commun.*, 1999, 673.
11 A. J. Koster, U. Zeise, A. J. Verkleij, A. H. Janssen, J. de Graf, J. W. Geus and K. P. de Jong, *Stud. Surf. Sci. Catal.*, 2000, **130**, 329.
12 A. J. Koster, U. Zeise, A. J. Verkleij, A. H. Janssen and K. P. de Jong, *J. Phys. Chem. B*, 2000, **104**, 9368.
13 B. Lee, D. Lu, J. N. Kondo and K. Domen, *Chem. Commun.*, 2001, 2118.
14 B. Lee, T. Yamashita, D. Lu, J. N. Kondo and K. Domen, *Chem. Mater.*, 2002, **14**, 867.
15 K. Zhu, B. Yue, W. Zhou and H. He, *Chem. Commun.*, 2003, 98.